Fourier transform photoemission spectroscopy

Meinders, M.B J; Drabe, K.E.; Jonkman, H.T.; Sawatzky, G.A

Published in:
Journal of Electron Spectroscopy and Related Phenomena

DOI:
10.1016/0368-2048(95)02377-1

ELSEVIER

Journal of Electron Spectroscopy and Related Phenomena 77 (1996) 1–6

JOURNAL OF ELECTRON SPECTROSCOPY and Related Phenomena

Fourier transform photoemission spectroscopy

M.B.J. Meinders*, K.E. Drabe, H.T. Jonkman, G.A. Sawatzky

Material Science Centre, Department of Solid State and Applied Physics, University of Groningen, Nijenborgh 4, 9747 AG Groningen, The Netherlands

First received 1 March 1995; accepted in final form 15 June 1995

Abstract

It is shown that photoemission spectra can be obtained by exciting the electrons with two phase-correlated wave trains. The phase-correlated wave trains are obtained by sending broad-band ultra-violet light, coming from a deuterium lamp, through a Michelson interferometer. It is possible to stabilize the interferometer within 20 nm on a time scale of a few minutes and is realized without active stabilization. The Fourier transform of the time-dependent electron yield from a polycrystalline silver sample is almost identical to the spectrum determined with the monochromator.

Keywords: Fourier transform spectroscopy; Phase-correlated wave train; Photoelectron spectroscopy

1. Introduction

In a search for new (angle-resolved) ultra-high energy resolved photoemission techniques, we investigate the possibility of exciting electrons by means of two broad-band phase-correlated wave trains, generated with a Michelson interferometer. In this way a interferogram of the emitted electrons is obtained as a function of the delay time between the two phase-correlated wave trains. The delay time corresponds to the relative displacements of the mirrors in the interferometer. The total photoemission spectrum as a function of incoming photon energy can now be reconstructed from the interferogram by means of a Fourier transform.

In infrared optics, Fourier transform spectroscopy is widely used because it has advantages over conventional methods. It is much less wasteful of light and may yield better energy resolutions. The product of throughput multiplied by energy resolution is one to two orders of magnitude larger for a Michelson interferometer than for a monochromator. This is because in a Fourier transform experiment one uses all frequencies simultaneously.

2. Basic principles of Fourier transform photoemission spectroscopy

The conventional way to obtain the total amount of emitted electrons as a function of incoming photon energy is to use a monochromator to select a single frequency from the output of a broad-band ultra-violet (UV) light source. The light is directed onto the sample and the number of emitted electrons is counted for that particular photon energy $\hbar\omega$. This procedure is repeated for several photon energies, yielding the photoemission spectrum

* Corresponding author.

SSDI 0368-2048(95)02377-1

$I_{PES}(\omega)$, as schematically shown in the left part of Fig. 1.

For small light intensities $I_L(\omega)$, the measured photoemission intensity in the single-particle picture is proportional to it and can be written as [1]

$$I_{PES}(\omega) \propto I_L(\omega) \sum_{i,f} w_{fi}(\omega) \tag{1}$$

where

$$w_{fi}(\omega) = \frac{2\pi}{\hbar} |\langle \psi_f | H^{int} | \psi_i \rangle|^2 \delta(E_f - E_i - \hbar\omega) \tag{2}$$

is the transition probability for an optical excitation between two single-electron states. The initial state ψ_i and final state ψ_f, having eigenenergies E_i and E_f, respectively, are eigenstates of the same Hamiltonian $H_0 = \mathbf{p}/2m + V(\mathbf{r})$. The interaction with the incident photons with energy $\hbar\omega$ is described by H^{int}.

An alternative method to obtain the spectrum is by measuring the photoelectron yield when the sample is irradiated with two phase-correlated UV-light beams. The phase delay between the beams is achieved by sending the output of the light source through a Michelson interferometer (see right part of Fig. 1). The beam splitter, coated on one side, divides the bundle into two parts. One bundle is reflected towards a mirror, where it is reflected back towards its former direction, and then partially transmitted by the beam splitter again. The other bundle is first transmitted by the beam splitter, reflected back by a movable mirror and finally partially reflected by the beam splitter. In this way, two wave trains are obtained with a phase difference determined by their travelled path difference $\Delta d = 2d_2 - 2d_1$. This optical path difference is also called the retardation.

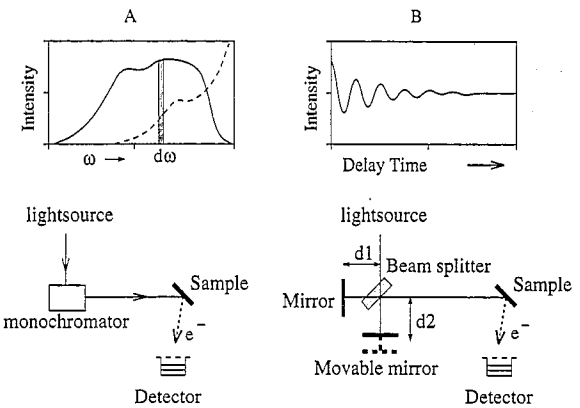

Fig. 1. (A) Schematic overview of a conventional measurement. The solid line is the intensity of the light source out of which the monochromator selects a frequency ω with a spread of $d\omega$. The dashed line shows the photoelectron spectrum obtained by scanning the monochromator. (B) Schematic overview of a Fourier-transform experiment showing the photoelectron intensity measured as a function of the delay time of the movable mirror.

If the travelled path length for both beams is equal, the phase difference between the two beams is π. This because a π-phase change occurs in the beam which is externally reflected at the beam-splitter. If we define $\tau = (\Delta d - \lambda/2)/c$, the electromagnetic field at the sample $A(t,\tau)$ may be described as the sum of both wave trains leaving the interferometer, yielding

$$\begin{aligned} A(t,\tau) &= \int_0^\infty A(\omega)(e^{-i\omega t} + e^{-i\omega(t+\tau)})\, d\omega \\ &= \int_0^\infty A(\omega)(1 + e^{-i\omega\tau})\, e^{-i\omega t}\, d\omega \end{aligned} \tag{3}$$

The light intensity $I_L(\tau)$ as a function of the delay-time τ, is given by a time-average of $|A(t,\tau)|^2$. Assuming no phase correlation between different photon energies and each ω component of the signal to be independent of the others, yields

$$\begin{aligned} I_L(\tau) &\propto \int_0^\infty |A(\omega)(1 + e^{-i\omega\tau})\, e^{-i\omega t}|^2\, d\omega \\ &= \int_0^\infty (2 + 2\cos\omega\tau) I_L(\omega)\, d\omega \end{aligned} \tag{4}$$

where we have replaced $|A(\omega)|^2$ with the frequency-dependent light spectrum $I_L(\omega)$. For a monochromatic source, the intensity varies as $\cos\omega\tau$. For a light source with a finite band width, the modulation for τ much larger than the coherence length will be approximately zero, as sketched in the right part of Fig. 1. The coherence length can be regarded as the length of the wave train and may be defined as $\Delta s \approx 2\pi c/\Delta\omega$ where $\Delta\omega$ is approximately the full-width half-maximum of the light spectrum $I_L(\omega)$.

The total photoelectron yield $I_{PES}(\tau)$ as a function of the delay time τ between the two wave trains is just given by the incoherent sum of all individual

light intensities of a single photon energy $\hbar\omega$, yielding

$$I_{PES}(\tau) \propto \int_0^\infty (2 + 2\cos\omega\tau) I_L(\omega) I_{tt}(\omega)\, d\omega \qquad (5)$$

where $I_{tt}(\omega) = \Sigma_{i,f} w_{fi}(\omega)$ is the total transition intensity.

Therefore, the electron yield will also show oscillations as a function of the relative displacement of the mirrors in the Michelson interferometer.

When subtracting the constant background in the obtained delay-time dependent intensities in Eqs. (4) and (5) we may write the interference part as

$$F(\tau) = \frac{2}{\sqrt{2\pi}} \int_0^\infty f(\omega) \cos\omega\tau\, d\omega \qquad (6)$$

where $F(\tau)$ corresponds either to the light or electron interferogram and $f(\omega)$ to the spectra $I_L(\omega)$ or $I_L(\omega)I_{tt}(\omega)$, respectively, and rescaling the unimportant proportionality constants. The spectrum $f(\omega)$ can now be calculated by taking the cosine Fourier transform of the interferogram

$$f(\omega) = \frac{2}{\sqrt{2\pi}} \int_0^\infty F(\tau) \cos\omega\, d\tau. \qquad (7)$$

It should be noted that the calculated $f(\omega)$ is an even function, $f(\omega) = f(-\omega)$, which is unphysical because it exists for negative frequencies. By dividing the mathematical spectrum in an odd and even function, it is a straightforward exercise to show that the physical spectrum is equal to twice the calculated spectrum for $\omega \geqslant 0$.

It is seen that the interferogram is an even function. In practice, there are always some small misalignments of the Michelson interferometer yielding a not perfectly even function. A detailed discussion about Fourier transform spectroscopy can be found, for instance, in Ref. [2].

3. Experimental set-up

In Fig. 2 a schematic diagram of the experimental set-up is shown. The output of the deuterium lamp (Oriel Inc., Q-series, high irradiance lamp, $2 < \hbar\omega < 6.6$ eV) was sent through a Michelson interferometer. In order to obtain precise displacements of the movable mirror, a polarized HeNe laser beam with wavelength $\lambda = 632.8$ nm ($\hbar\omega = 1.96$ eV) was also mixed with the UV light. In connection with the output of the deuterium lamp, the laser beam was also used to align the optical components. Special attention was paid to the optical components to obtain a proper broad-band operation. A band-pass filter (200 to 500 nm, Oriel Inc., model 51666) was mounted after the deuterium lamp to suppress some strong lines in the red. These deuterium lines would otherwise interfere with the 632.8 nm line from the HeNe laser. After the filter, a polarizer was used to obtain *p*-polarized light. The aperture of the system was limited with diaphragms to such an extent that good contrast ratios were obtained at the reference photomultiplier (Thorn EMI, model 9558QB), used to measure the UV-light intensity (Pm1 in Fig. 2). The beam splitter of the Michelson interferometer was a quartz etalon (25 mm diameter, flatness $\lambda/3$), coated on one side with a dielectric multilayer. The reflectivity for *p*-polarized light is 50% at $\hbar\omega =$ 4.5 eV. Also an uncoated quartz etalon was mounted for compensation, in order to ensure that both reflected beams in the interferometer passes a quartz etalon three times. For *p*-polarized light, the reflectivity at the uncoated surfaces can be neglected. The end mirrors of the Michelson

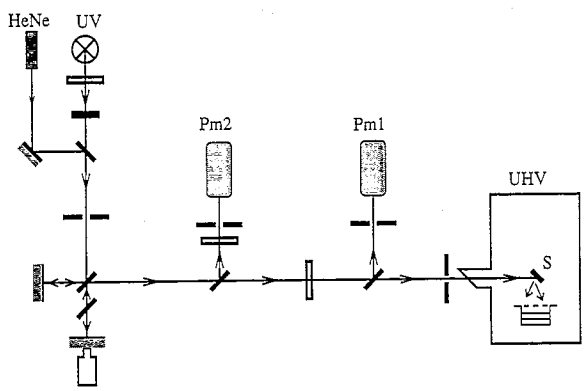

Fig. 2. Schematic overview of the experimental set-up. The output of the deuterium lamp (UV) and HeNe laser are sent through a Michelson interferometer. The interference patterns of the UV and HeNe are measured by photomultipliers 1 and 2, respectively. The light beam enters the ultra-high vacuum (UHV) system through a LiF window and is focussed on the sample. The emitted electrons are detected by means of a position-sensitive detector.

interferometer were protected UV-enhanced aluminium mirrors with a diameter of 25 mm and flatness of $\lambda/10$. The movable end mirror was mounted on a translational stage (Burleigh, model TS100) and was driven by an inchworm motor (Burleigh, model IW710; controller, model 6100). The discrete displacements of the motor are not constant but vary between 5.0 and 7.5 nm per single step. The precise displacement could be determined from the interference pattern of the HeNe beam.

The interferometer was not actively stabilized but the HeNe laser, deuterium lamp, interferometer and optical components in between were mounted on a 30×60 cm^2 optical breadboard (Photon Control). This breadboard was placed on a laboratory made optical table in between a ± 5 cm thick piece of polyurethane and a piece of bubble-wrap. All this was surrounded by wind shields. In this way the mirrors were stabilized within 10–20 nm on a time scale of a few minutes, while data accumulation took about one minute for each point. The long term drift of the Michelson interferometer was therefore not important because the absolute displacement between the two mirrors was calculated afterwards.

After passing the interferometer, the HeNe beam was spectrally and physically separated from the UV light and its light intensity was measured with another photomultiplier. After passing an iris diaphragm, the light beam entered the ultra-high vacuum (UHV) system through a LiF window. The pressure in the UHV system was between 10^{-9} and 10^{-10} Torr.

The emitted electrons were measured with a position-sensitive detector, consisting of two electron-multiplying microchannel plates (MCP) (25 mm diameter) and a resistive anode. Just above the MCPs, a molybdenum grid was mounted to control the voltage between sample and detector. The bias voltage between the Mo grid and the first MCP is about 100 V to ensure that electrons hitting the MCP surface have sufficient energy to cause an electron avalanche and will be counted.

4. Experimental results and discussion

The experiments were performed on a polycrystalline silver sample at room temperature. It was cut from 99.999% pure silver rod and mirror polished before introducing it into the UHV chamber. Prior to the experiments, a clean surface was obtained by sputtering the sample with argon ions (500 eV) for several minutes.

The intensity of the HeNe beam, UV beam and the total electron current coming from the polycrystalline silver sample, were recorded simultaneously as a function of the mirror displacement. A typical example of the measured intensities are shown in the left part of Fig. 3. From the interference pattern of the HeNe beam it can be clearly seen that the displacement of the mirror is not constant. The inchworm motor consist of three piezo elements, two at the end which are used to clamp the elements at the surrounding shaft, and one in the middle to bring about the displacement of the mirror. After a maximal (minimal) displacement, a clamp change between the piezo elements at the front and at the back is realized. This procedure causes a large uncertainty in the actual displacement as can be seen near steps number 200 and 700. Furthermore it can be seen that between the clamp changes, the displacement of the middle piezo element is not linear with respect to the applied voltage. The displacement varies between 50 and 75 Å per step.

Because the actual displacement between a

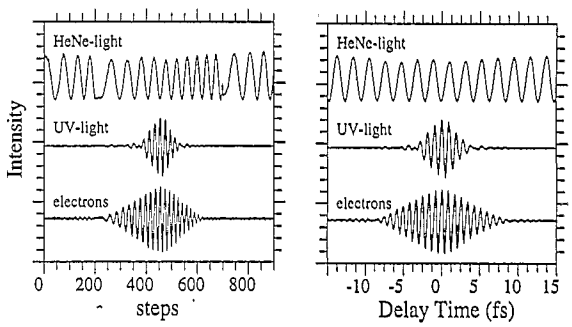

Fig. 3. (Left) The measured intensities coming from the two photomultipliers (HeNe light and UV light) and the measured electron yield coming from the polycrystalline silver sample. The number of steps performed by the inchworm motor is on the horizontal axis. (Right) Same, but corrected for the actual relative displacement between the two mirrors of the Michelson interferometer. The horizontal axis now corresponds to the delay time between the phase correlated wave trains of the HeNe and UV light.

maximum and a nearest-neighbour minimum of the HeNe interference pattern is equal to $0.5\lambda_{HeNe} = 3164$ Å, the actual delay time (about 1.055×10^{-15} s) between the two phase-correlated UV wave fronts is easily calculated. The corrected spectrum is shown in the right part of Fig. 3, and it is seen that nice interference patterns are obtained. The interference pattern of the HeNe light shows a small modulation due to the finite coherence length.

The coherence length of the UV light is roughly half the total length of the pulse train. The length of the pulse train corresponds to the length of the interference pattern of the UV light measured. It can now be seen that the coherence time of the UV light source is about $\Delta t \approx 2 \times 10^{-14}$ s, corresponding to a coherence length of $\Delta l \approx 1$ μm and band width of approximately $\Delta E = \hbar\Delta\omega = h/\Delta t \approx 1$ eV.

The electrons will only be emitted for $\hbar\omega$ larger than the work function Φ. In the electron spectrum one effectively sees the coherence time of the light that is modified by the photoemission threshold. Because this threshold is roughly equal to the central frequency of the UV light, the coherence time of the light after the interaction with the solid would be approximately twice as long, indicating a band width of 0.5 eV.

The Fourier transform of the interference patterns of the UV light and emitted electrons, as shown in the right part of Fig. 3, are plotted in Fig. 4. The spectra are obtained by means of a discrete fast Fourier transform (FFT) routine with 25 meV resolution. Also shown is a photoemission spectrum of polycrystalline silver (square points) as measured with the monochromator. Both electron spectra are already corrected for light-intensity variations.

It is seen that near the electron escape threshold the spectra look very similar, while in the high photon-energy region deviations occur. However, we established that light-intensity corrections, especially for the experimental set up with the monochromator, cannot be fully trusted for large photon energies [3]. Their origin is not fully understood. However, they have not been investigated in detail because we have been, up to now, mainly interested in the photoelectric yield in a small energy region around the electron escape threshold.

The electron spectra may be explained by the surface-photoemission description (one-step model) with a constant matrix-element approximation [3–7]. Due to momentum conservation parallel to the surface of the sample, very low count rates near the electron escape threshold are

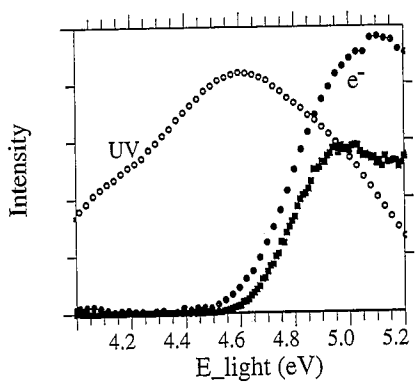

Fig. 4. UV-light intensity (○) and near-threshold photoelectron current (●) obtained by Fourier transforming the interference patterns shown in Fig. 3. A near-threshold photoemission spectrum from polycrystalline silver (■) is also shown which has been measured by filtering the UV light with a monochromator. The electron spectra are corrected for light intensity.

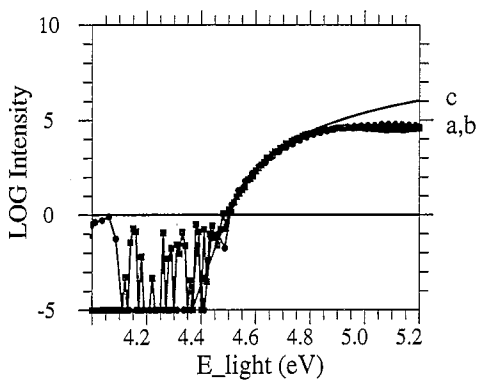

Fig. 5. The logarithm of the near-threshold photoelectron yield of polycrstalline Ag at $T \approx 300$ K (lines a and b), obtained with the Michelson interferometer ● and monochromator (■) (see also Fig. 4). The spectrum measured with the monochromator is also shifted 40 meV to lower photon energies which accounts for the difference in work function between the samples. Also shown is the constant matrix-element approximation for a free-electron like metal (c).

obtained. To analyse the data, better sensitivity in this region is obtained by taking the logarithm with respect to the measured electron yield. This so-called Fowler plot [7] is shown in Fig. 5, after the experimental spectra were corrected for background intensity. Also shown is the expected yield of a free-electron like material. The experimental curves are shifted vertically by an unimportant scaling factor. The spectrum measured with the monochromator is also shifted 40 meV to lower photon energies which accounts for the difference in work function of both samples. From Fig. 5 it can be seen that the near-threshold photoelectron spectrum measured with the monochromator and measured with the Michelson interferometer yield almost identical results.

5. Conclusions

In order to make use of the advantages of Fourier transform spectroscopy, we investigated the possibility of performing photoemission spectroscopy (PES) by exciting the electrons from the solid into the vacuum with two phase-correlated wave trains. We made use of a deuterium lamp emitting photons in the energy range 2–6.8 eV. The output was sent through a Michelson interferometer and directed onto a polycrystalline silver sample while the emitted electrons were counted as a function of the delay time between the two phase-correlated wave trains.

We showed that it was possible to stabilize the Michelson interferometer within 20 nm, for several minutes. This was obtained without active stabilization. The measurement time for one particular delay time was a few minutes. The long-term drift of the interferometer and the actual displacement of the movable mirror which was driven by an inchworm motor, could be calculated afterwards based on the interference pattern of a HeNe laser beam, which was mixed with the UV output.

In this way, nice interference patterns were obtained of the HeNe beam, UV beam and electron yield. The Fourier transform of the interferogram yields a spectrum almost identical to the photoemission spectra obtained by monochromatizing the UV output and counting the escaping electrons for every photon energy separately.

Because the Michelson interferometer was stabilized using very simple means, it may be expected that, using active stabilization, the stability of the interferometer could be improved by a factor of 10 or 20. This implies that Fourier transformed photoemission experiments may be possible up to 50 or 100 eV, provided that suitable mirrors and beamsplitters can be found in this energy region. Furthermore, it should be possible to obtain a stable interferometer with a maximum retardation of 1 mm. Considering that the resolution is approximately equal to the inverse of the maximum retardation, it may be expected that a resolution of about 1 meV could be obtained using this technique.

References

[1] C.O. Almbladh and L. Hedin, E.E. Koch (Ed.), in Handbook on Synchrotron Radiation, Vol. 1, North Holland Publishing Company, Amsterdam 1983, Chap. 8.
[2] J. Chamberlain, The Principles of Interferometric Spectroscopy, John Wiley and Sons, 1979.
[3] M.B.J. Meinders, Low-energy spectral weights in correlated systems, Ph.D. Thesis, University of Groningen, 1994.
[4] K. Mitchell, Proc. R. Soc. Lond. Ser. A, 146 (1934) 442.
[5] I. Adawi, Phys. Rev., 134 (1964) A788.
[6] G.D. Mahan, Phys. Rev. B, 2 (1970) 4334.
[7] R.H. Fowler, Phys. Rev., 38 (1931) 45.